

Diffraction Radiation Oscillator with Frequency Tuning on Mutual Coupled Modes in an Open Resonant System

Ievgen O. Kovalov*, Vladimir S. Miroshnichenko, and Yelena B. Senkevich

Abstract—The results of experimental research and development of the diffraction radiation oscillator with a periodic structure in form of a reflective double comb and with frequency tuning on mutual coupled modes in its open resonant system were presented. As an operating mode we chose the mutual coupled modes $TEM_{002} \leftrightarrow TEM_{101}$, which arise in the open resonant system with the shift between mirrors symmetry planes. To analyse its features, a rigorous electro-dynamical 2-D model of the open resonant system was used, and the optimal shift width was established. As a result, the operation on the mutual coupled modes allowed to extend the frequency tuning range without failures in output power and to exclude the influence of higher-order modes (TEM_{20q} , TEM_{30q} etc.) on the output characteristics of the oscillator. The research has been carried out in K_a band.

1. INTRODUCTION

In powerful diffraction radiation oscillator (DRO) an open resonant system (ORS) with a periodic structure in form of a metallic double comb is used, which is placed on the ORS mirror [1–3]. The operating mode in the ORS (TEM_{00q} or TEM_{20q}) provides in-phase excitation of all double comb slots, and a sheet electron beam transfers its energy to the resonant field when moving in a spatially periodic field in a channel of the double comb. The tuning of oscillation frequency (f) in DRO on the operating mode is provided by synchronous changes in accelerating voltage for the electron beam and in a resonant distance between the ORS mirrors ($D_{00q}(f)$ or $D_{20q}(f)$). Limited by the width double comb turns the mirror into a two-level reflective surface. This leads to a significant difference in the slope of the dispersion curves $D_{mnq}(f)$ for operating and higher-order modes in the ORS. At the intersection or approaching of the dispersion curves for operating and higher-order modes, the decrease of an output power of DRO occurs, and even there is a failure of an oscillation as a result of a mutual coupling of the ORS modes [4, 5]. However, there are a lot of successful applications of mutual coupled modes in RF/microwave devices, such as narrow-band bandpass filters for mobile communications systems [6], highly resonant wireless power transfer adapters [7], etc.

Developed rigorous spectral theory for the analysis of excited modes in an open resonators (OR) [8], as well as research methods of the Morse critical points (MCP) for the relevant dispersion equations [9], allowed to identify and examine in detail the mutual coupled modes in OR with cylindrical and spherical mirrors. Thus, it was found that: the OR modes of the same symmetry classes (by transverse indexes) come into mutual coupling near MCP; the dispersion equation for the partial resonant frequencies near MCP can be described by quadratic form for the spectral and geometrical parameters of the OR; and the dispersion curves $D(f)$ for mutual coupled modes near MCP are similar to Wien's plots for coupled resonant circuits.

Received 21 June 2018, Accepted 31 August 2018, Scheduled 8 September 2018

* Corresponding author: Ievgen O. Kovalov (kovalov.ievgen@gmail.com).

The authors are with the O.Ya. Usikov Institute for Radiophysics and Electronics, National Academy of Sciences of Ukraine, 12, Akad. Proskury str, Kharkiv 61085, Ukraine.

There is always a small asymmetry in the relative position of mirrors in experimental prototypes of DRO with sphero-cylindrical or hemispherical ORS [1, 2]. This leads to additional mutual coupling of modes with different classes of symmetry on transverse indexes. Thus, in the small-sized DRO due to a slight displacement of the mirrors symmetry planes, a local mutual coupling between TEM_{002} and TEM_{101} -modes was observed. It was accompanied by a decrease in ORS Q-factor and failure in the output power of DRO [10]. The creation of conditions for the mutual coupling between the operating (fundamental) TEM_{00q} -mode and the nearest TEM_{10q-1} -mode, which still has a high quality factor, will make possible the DRO operation on the mutual coupled modes in a wide frequency range. Thereby, we can diminish the higher-order modes influence (TEM_{20q} , TEM_{30q} , TEM_{40q} , etc.) on the output characteristics of the oscillator.

The purpose of the present paper is to study the features of the mutual coupled modes in the ORS with a periodic structure in form of the reflective double comb; to choose the optimal shift between the mirrors symmetry planes for the extension of DRO frequency tuning range on mutual coupled modes; and to study the features of DRO, operating on the mutual coupled modes in “hot” regime. The research has been carried out in K_a band.

2. FEATURES OF THE MUTUAL COUPLED MODES IN A 2-D MODEL OF THE ORS WITH THE DOUBLE COMB

Consider a hemispherical ORS with the reflective double comb, placed in the centre of the flat mirror (Fig. 1). The following designations of ORS parameters were used: R_{sph} — the curvature radius of the spherical mirror; $2A$ — the spherical mirror aperture; D — the distance between mirrors; l — the period and d — the width of the double comb slots; L — the length of the double comb along OY ; δ — the width of the channel between combs; a — the total width of the double comb along OX ; b — the height of the double comb along OZ ; s — the width of the shift between mirrors symmetry planes along OX . To excite the oscillations in DRO with such ORS, the sheet electron beam is used, which is moving in the channel between the combs and interacts with the electric component of the operating mode field (TEM_{00q} or TEM_{20q}). A large number of higher-order modes excites in the ORS when DRO operates on the TEM_{00q} -mode with a longitudinal index $q = 4 \div 6$. This complicates the analysis of the mutual coupling of modes. Therefore, we studied the features of the ORS with a minimum distance between mirrors, where is only the operating TEM_{002} -mode with a single field variation between mirrors, and a single field variation in the double comb, and the first higher-order mode is TEM_{101} .

The mutual coupling features of TEM_{002} and TEM_{101} -modes at shift $s \neq 0$ were considered using a rigorous 2-D model of the ORS, in which the mirrors are thought of as parallel, infinitely thin, perfectly conducting, extending infinitely and uniformly along OY . The double comb was designed as a rectangular groove on a flat mirror. The width and depth of the rectangular groove (a and b)

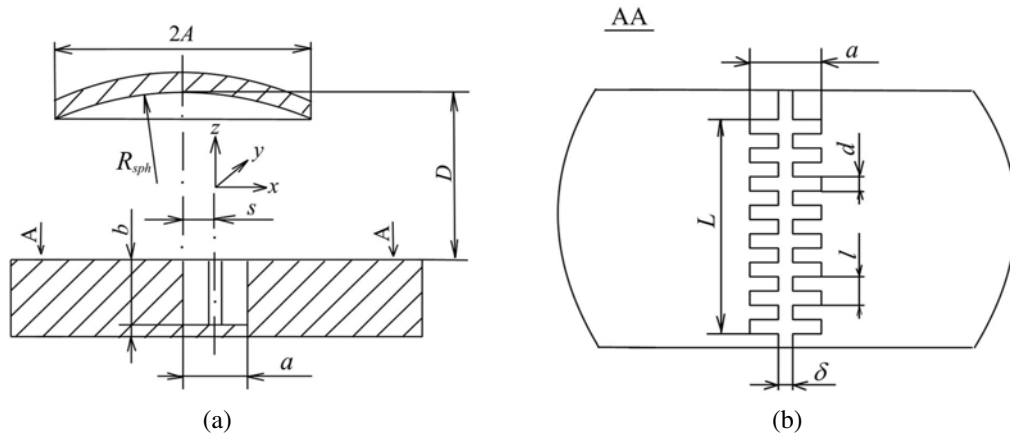


Figure 1. Schematic of the ORS with periodic structure in form of reflective double comb: (a) front view of the ORS; (b) top view on the flat mirror.

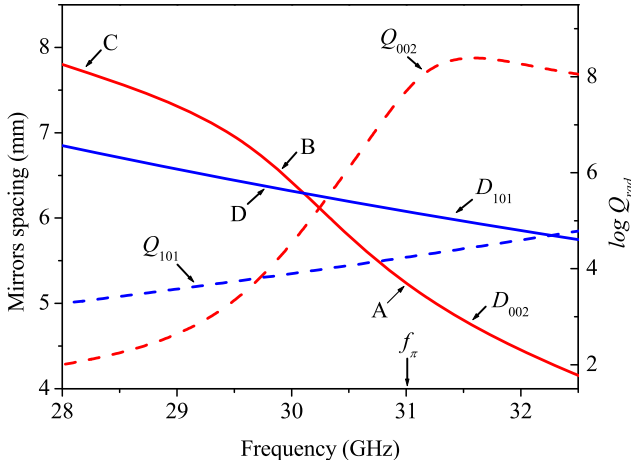


Figure 2. Dispersion diagram $D(f)$ and radiation Q-factor $Q_{rad}(f)$ for TEM_{002} and TEM_{101} -modes, calculated using the rigorous 2-D model of symmetric ORS with rectangular groove on the flat mirror.

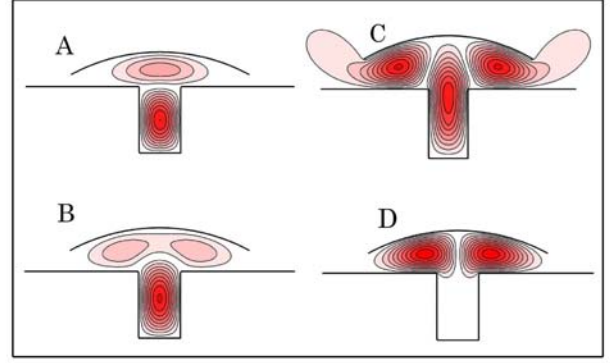


Figure 3. The E_y -field distribution at the points A, B, C, D of dispersion curves, shown on Fig. 2.

corresponded to the width and height of the double comb (the case of E-polarization for resonant field was considered — $\vec{E} \parallel OY$) [11]. To analyze the features of mutual coupled modes was used the small-sized ORS with the following parameters: $R_{cyl} = 22.5$ mm — the curvature radius of cylindrical mirror; $2A = 24$ mm — the aperture of cylindrical mirror along OX ; the aperture of flat mirror along OX — 36 mm; $a = 5.524$ mm; $b = 10.0$ mm. The resonant frequency for full matching of the groove with the ORS field was:

$$f_{\pi} = \frac{c}{2b} \sqrt{1 + \left(\frac{2b}{\lambda_{cr}}\right)^2} = 31.0218 \text{ GHz} \quad (1)$$

where c is the speed of light in vacuum, $\lambda_{cr} \approx 2a$ — the critical wavelength of fast H_{10} -wave that propagates in the double comb along OZ [12]. The change of the shift s between the mirrors symmetry planes in this ORS allowed to control the value of mutual coupling between the even TEM_{002} -mode and odd TEM_{101} -mode.

Consider the features of TEM_{002} and TEM_{101} -modes, exited in the symmetric ORS with the rectangular groove on the flat mirror and perfect conductivity of mirrors. As a result of H_{10} -wave elongation in the rectangular groove, the slope of dispersion curve $D_{002}(f)$ for TEM_{002} -mode was higher, than the slope of dispersion curve $D_{101}(f)$ for TEM_{101} -mode (Fig. 2). At frequency tuning on the operating TEM_{002} -mode, the significant change of the resonant field structure for E_y -component was observed (see fields A, B, C on Fig. 3). On the lower frequencies of tuning range, the mutual coupling of even modes $TEM_{002} \leftrightarrow TEM_{201}$ was observed, accompanied by decreasing of radiation Q-factor in the ORS to $\log(Q_{rad}) = 2 \div 3$. The resonant field of the odd TEM_{101} -mode didn't penetrate into the rectangular groove, and its field structure didn't change over the frequency tuning range (see field D on Fig. 3). Near the crossover point of dispersion curves $D_{002}(f)$ and $D_{101}(f)$ (at $f = 30.107$ GHz, $D = 6.29$ mm), the local change of Q-factor for TEM_{002} and TEM_{101} -modes was not observed. I.e., there is no interaction between TEM_{002} and TEM_{101} -modes in the symmetric ORS.

The crossover point of dispersion curves for TEM_{002} and TEM_{101} -modes in the symmetric ORS (Fig. 2) corresponds to coordinates of MCP (f_{MCP} , D_{MCP}) for dispersion equation of mutual coupled modes $TEM_{002} \leftrightarrow TEM_{101}$ that arise in the ORS at a parallel shift of mirrors symmetry planes. In case of the 2-D model of the ORS, the dispersion equation for the mutual coupled modes $TEM_{002} \leftrightarrow TEM_{101}$, which includes real part of spectral parameters f and f_{MCP} and non-spectral parameter D , can be expressed in the form:

$$(D - D_{mid})^2 - \xi^2 (f - f_{MCP})^2 - (\psi s)^2 = 0 \quad (2)$$

where $D_{mid} = D_{MCP} + \frac{1}{2} \left(\frac{\partial D_{002}}{\partial f} + \frac{\partial D_{101}}{\partial f} \right) (f - f_{MCP})$, $\xi = \frac{1}{2} \left(\frac{\partial D_{002}}{\partial f} - \frac{\partial D_{101}}{\partial f} \right)$, $(\psi s)^2$ — the value of modes mutual coupling in the ORS with the shift between mirrors symmetry planes $s \neq 0$.

Parameters $\partial D_{002}/\partial f$ and $\partial D_{101}/\partial f$ can be defined by dispersion curves $D_{002}(f)$ and $D_{101}(f)$ for symmetric ORS at $f = f_{MCP}$. The coupling parameter $\psi = \frac{\partial D_{002} \leftrightarrow 101}{\partial s}$ can be defined by change of the resonant distance $D(f_{MCP})$ for the branches of $TEM_{002} \leftrightarrow TEM_{101}$ at $s \rightarrow 0$.

In Fig. 4(a), the dispersion curves $D(f)$ for the mutual coupled modes $TEM_{002} \leftrightarrow TEM_{101}$ are shown, which was found using the rigorous 2-D model of the ORS with the rectangular groove on the flat mirror at $s = 0.2$ mm; 1.0 mm; 2.45 mm. On the dispersion diagram near MCP ($f_{MCP} = 30.107$ GHz, $D_{MCP} = 6.29$ mm), the zone of the mutual coupled modes $TEM_{002} \leftrightarrow TEM_{101}$ with the lower and upper branches for partial frequencies was formed. It extended with increasing of the shift (s) between mirrors symmetry planes. To obtain the dispersion branches of the mutual coupled modes $TEM_{002} \leftrightarrow TEM_{101}$, using Equation (2), the necessary parameters were found at dispersion curves analysis in the symmetric ORS: $\partial D_{002}/\partial f = 1.267$ mm/GHz; $\partial D_{101}/\partial f = 0.246$ mm/GHz. The calculated parameter ψ didn't change for $0 < s < 1.2$ mm and was $\psi = 0.22$. The approximation results of the dispersion branches, using Equation (2) are shown in dots in Fig. 4(b). As can be seen, near MCP they are in a good agreement with the dispersion curves, obtained using rigorous 2-D model.

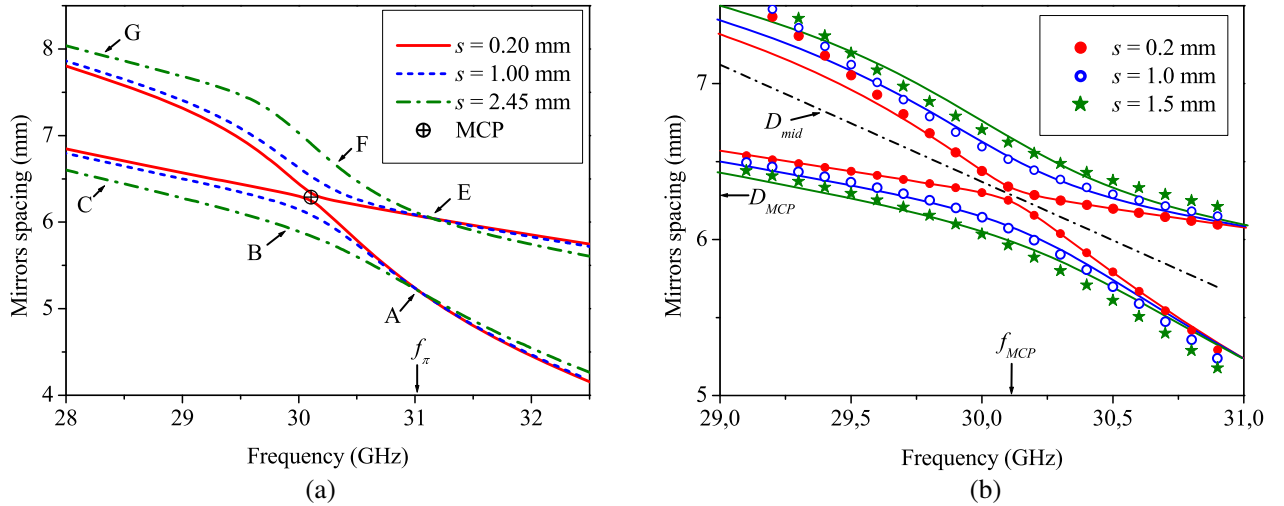


Figure 4. Dispersion diagram for the mutual coupled modes $TEM_{002} \leftrightarrow TEM_{101}$ in the ORS at the shift s between mirrors symmetry planes: (a) dispersion branches calculated using 2-D model of the ORS; (b) dispersion branches approximation (dots) according to the equation (2).

The features of the resonant field distribution (E_y -component) at frequency tuning on the lower and upper branch of the mutual coupled modes at $s = 2.45$ mm is shown in Fig. 5. The tuning down the resonant frequency on the lower branch of the mutual coupled modes $TEM_{002} \leftrightarrow TEM_{101}$ was accompanied by the transformation of the field structure from TEM_{002} to TEM_{101} -mode (see fields A, B, C in Fig. 5). At the tuning down the frequency on the upper branch of the mutual coupled modes $TEM_{002} \leftrightarrow TEM_{101}$, the transformation of the field structure from $TEM_{101+001}$ to TEM_{201} -mode was observed (see fields E, F, G in Fig. 5). The significant level of the resonant field in the rectangular groove made possible the excitation of oscillations in DRO (when filling the groove by the double comb) both on the lower and upper branches of mutual coupled modes $TEM_{002} \leftrightarrow TEM_{101}$.

Consider the features of energy exchange between TEM_{002} and TEM_{101} modes when $s \neq 0$. At the small shift between mirrors symmetry planes ($s = 0.20$ mm), there was abrupt decreasing of Q-factor near f_{MCP} on the lower branch of mutual coupled modes (Fig. 6(a)). On the upper branch of mutual coupled modes, it was a local increase of Q_{rad} (Fig. 6(b)). This was caused by energy exchange between the mutual coupled modes with close frequencies. When the shift between mirrors symmetry planes increased ($s = 1.0$ mm, $s = 2.45$ mm), the frequency spacing for lower and upper branches of the mutual

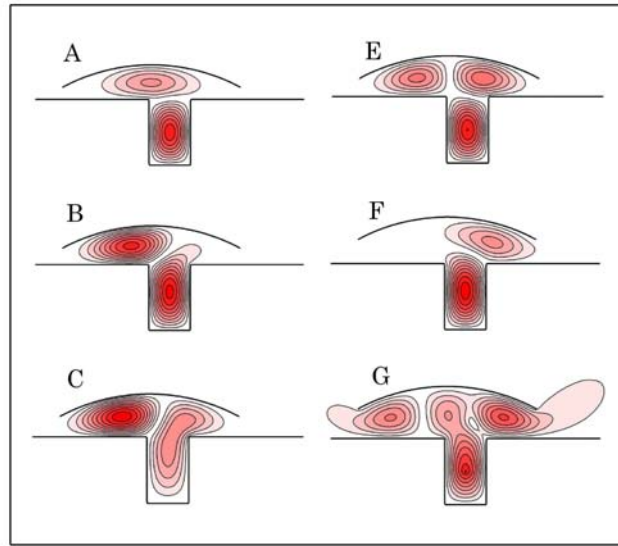


Figure 5. The E_y -field distribution in the ORS with $s = 2.45$ mm at the points A, B, C, E, F, G of the dispersion diagram, shown on Fig. 4(a).

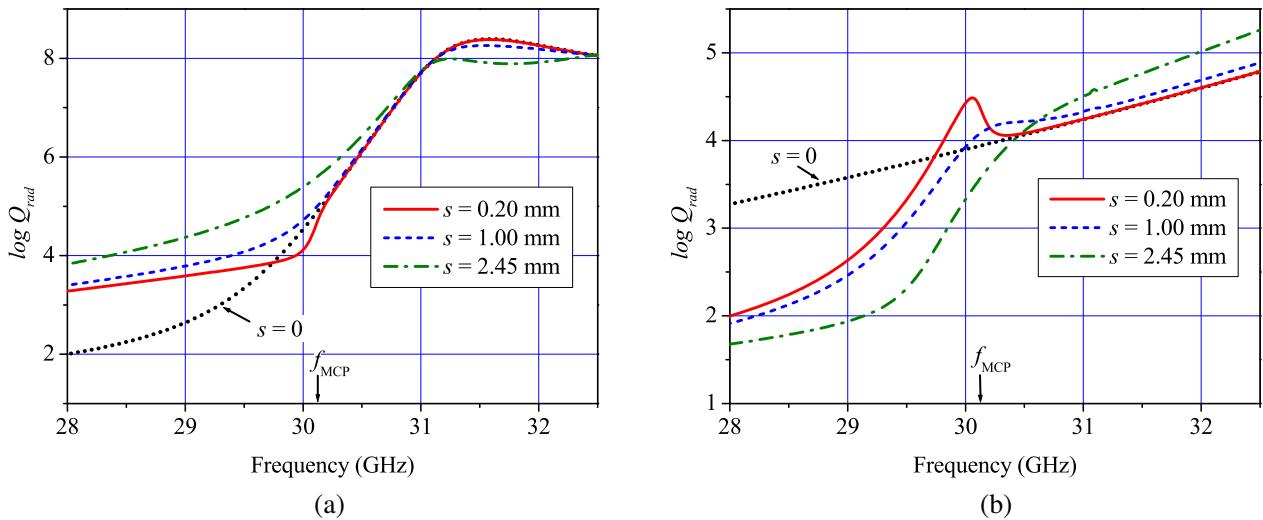


Figure 6. Behavior of $Q_{rad}(f)$ of in the ORS with rectangular groove on the mirror at frequency tuning on the lower branch (a) and on the upper branch (b) of the mutual coupled modes $TEM_{002} \leftrightarrow TEM_{101}$.

coupled modes at $D = const$ significantly exceeded the width of both resonances in the ORS, and modes exited independently, without energy exchange. Due to change of the resonant field structure at tuning down the frequency on the lower branch of the mutual coupled modes, there was a significant increase in Q-factor up to $\log(Q_{rad}) > 4$ on frequencies $f < f_{MCP}$ (Fig. 6(a)), which at $s = 2.45$ mm gave the opportunity to extend the frequency tuning range of DRO, operating on the mutual coupled modes. On the upper branch of mutual coupled modes at $s = (1.0 \div 2.45)$ mm, the decreasing of Q_{rad} at $f < f_{MCP}$ in comparison with symmetric ORS was observed (Fig. 6(b)).

When the rectangular groove was filled by the double comb, the slope of $D_{002}(f)$ decreased, and the zone of the modes mutual coupling shifted down the frequency range. Thus, when the used parameters of the double comb were $a = 5.58$ mm, $b = 10.0$ mm, $l = 1.0$ mm, $d = 0.5$ mm, $\delta = 0.2$ mm, the frequency for full matching of the double comb (1) slightly changed — $f_{\pi} = 30.904$ GHz. The crossover point of

dispersion curves for TEM_{002} and TEM_{101} modes in the symmetric ORS with the double comb was shifted down the frequency range to $f_{MCP} = 29.415$ GHz.

For the mutual coupled modes $TEM_{002} \leftrightarrow TEM_{101}$ in the ORS with the double comb, the total Q-factor (Q_{total}) was obtained. It included radiation loss ($1/Q_{rad}$) and ohmic ($1/Q_{ohm}$) loss in mirrors surface (copper conductivity — $\sigma = 5.8 \times 10^7$ Sm/m):

$$Q_{total} = (1/Q_{rad} + 1/Q_{ohm})^{-1} \quad (3)$$

It was found that the resonant frequency tuning on the lower branch of the mutual coupled modes $TEM_{002} \leftrightarrow TEM_{101}$ at the shift between mirrors symmetry planes $s = (0.5 \div 2.5)$ mm was accompanied with the increasing of Q_{total} on frequencies $f < f_{MCP}$ (Fig. 7(a)). For the upper branch of the $TEM_{002} \leftrightarrow TEM_{101}$ was observed the decreasing of Q_{total} even at $f > f_{MCP}$, which was caused by the resonant field penetrating into the double comb (Fig. 7(b)).

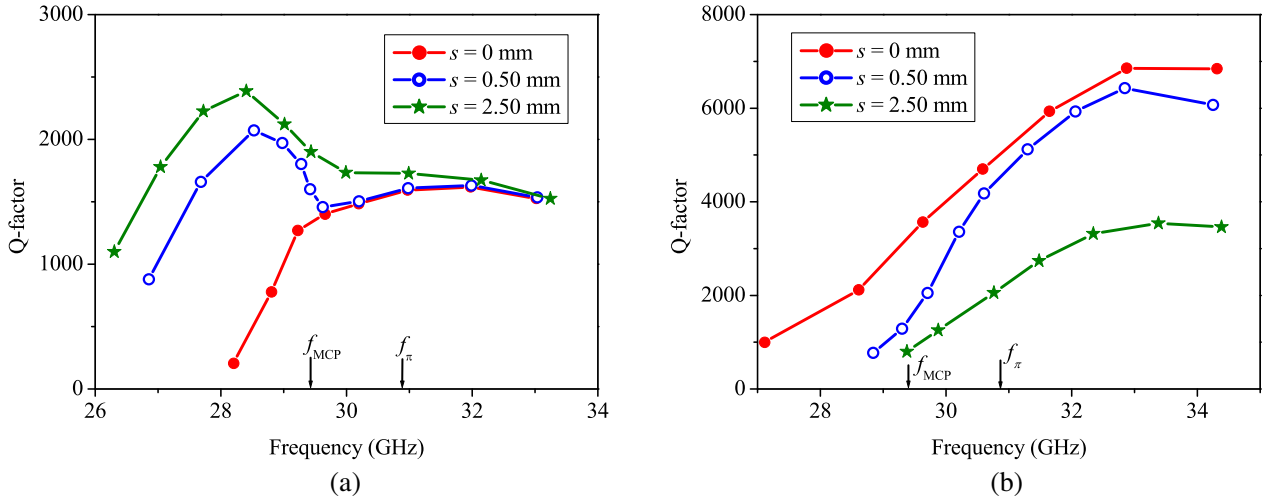


Figure 7. Behavior of the total Q-factor in the ORS with the double comb at frequency tuning on the lower branch (a) and on the upper branch (b) of the mutual coupled modes $TEM_{002} \leftrightarrow TEM_{101}$.

The starting currents analysis for excitation of oscillations in DRO, operating on the mutual coupled modes $TEM_{002} \leftrightarrow TEM_{101}$, was carried out for 2-D model of the ORS with the above parameters of the double comb and interaction space length $L = 10$ mm $\approx 2\omega_0$ ($2\omega_0$ — field spot diameter for TEM_{002} -mode on the flat mirror and with spherical mirror radius $R_{sph} = 22.5$ mm).

The calculation of the starting current was implemented using the results of the linear theory of DRO [13] for the case of the small space charge in the electron beam and homogeneous distribution of the resonant field throughout the interaction space:

$$I_{start}(f) = \frac{8.14 \cdot 10^{-5} S_{beam} U^{3/2}}{\zeta Q L^2} \quad (4)$$

where, U — accelerating voltage that satisfies the synchronism of the electron beam with the 1st space harmonic of the periodic field in the double comb; $\zeta = \frac{S_{beam} \int E_{1,y}^2 ds}{\int_{S_{ORS}} E_y^2 ds}$ — the utilization coefficient of the resonant field; Q — the total Q-factor of the ORS; S_{beam} — cross-section area of the sheet electron beam, S_{ORS} — cross-section area of the ORS.

The required parameters ζ and Q were found, when we analyzed the features of the mutual coupled modes in 2-D model of the ORS with the double comb and $S_{beam} = \omega 0.2 \times 10$ mm². The results of starting current calculation are shown in Fig. 8. At the shift between mirrors symmetry planes $s = 2.5$ mm, the zone of mutual coupled modes existence extended. This contributed to significant reduction of starting current at DRO tuning down the frequency on the lower branch of mutual coupled modes at

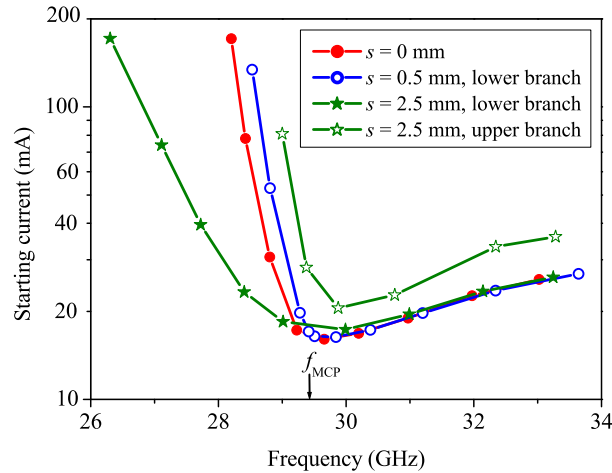


Figure 8. The starting current of the DRO versus f at frequency tuning on the TEM_{002} -mode in symmetric ORS ($s = 0$), and on the mutual coupled modes $TEM_{002} \leftrightarrow TEM_{101}$ at $s = 0.5$ mm and $s = 2.5$ mm.

$f_{cr} < f < f_{MCP}$, where $f_{cr} \approx c/2a = 26.88$ GHz — cutoff frequency of the H_{10} wave in a double comb array [12]. At DRO tuning on the upper branch of the mutual coupled modes $TEM_{002} \leftrightarrow TEM_{101}$, the calculated value of starting current at $f > f_{MCP}$ was only 1.5–2 times larger than the starting current of DRO on the lower branch of mutual coupled modes.

3. EXPERIMENTAL STUDY OF THE MUTUAL COUPLED MODES FEATURES IN THE ORS WITH THE DOUBLE COMB

The research of the mutual coupled modes features has been carried out on the model of a small-sized ORS (Fig. 1), which consisted of the spherical mirror of curvature radius $R_{sph} = 22.5$ mm and round aperture of diameter $2A = 28$ mm. The coupling unit of the ORS with waveguide was made in form of a wedge-shaped junction to the slot 0.1×7.2 mm², which was placed in the spherical mirror centre. The flat mirror aperture along OX and OY was 52×32 mm². The double comb was placed in the rectangular groove, its parameters were: $a = 5.58$ mm, $b = 10.0$ mm, $l = 1.0$ mm, $d = 0.5$ mm, $\delta = 0.2$ mm. The dispersion curves $D_{mnq}(f)$ and the ORS Q-factor on the mutual coupled modes were obtained by reflection coefficient measurements in the output waveguide [14].

The experimental dispersion curves for the TEM_{002} -mode in the symmetric ORS and for the mutual coupled modes $TEM_{002} \leftrightarrow TEM_{101}$ in the ORS with the shift between mirrors symmetry planes are shown in Fig. 9(a). The coordinates of MCP on the dispersion curve ($f_{MCP} = 29.41$ GHz, $D_{MCP} = 6.83$ mm) were found at the splitting zone of dispersion curve $D_{002}(f)$ at shift between mirrors symmetry planes $s \approx 0.1$ mm. When we increased the shift between mirrors symmetry planes, the zone of the mutual coupling extended, and the dispersion curve $D_{002}(f)$ divided into two branches of the mutual coupled modes $TEM_{002} \leftrightarrow TEM_{101}$. Due to the location of the coupling slot in the centre of the spherical mirror, we didn't detect the upper branch of the mutual coupled modes $TEM_{002} \leftrightarrow TEM_{101}$ on frequencies $f > 30.4$ GHz.

For the lower branch of the mutual coupled modes $TEM_{002} \leftrightarrow TEM_{101}$, the measurements of loaded Q-factor Q_{load} and the coupling coefficient of the ORS β have been carried out. These parameters determine the starting current for excitation of oscillations in DRO and effective output of generated power to the load. At the small shift between mirrors symmetry planes ($s = 0.5$ mm) the low-frequency tuning range on the mutual coupled modes was located near f_{MCP} and the abrupt decrease in parameters Q_{load} and β at $f \rightarrow f_{MCP}$ was observed (Fig. 9(b), Fig. 9(c)). The increasing of the shift between mirrors symmetry planes to $s = (1.5 \div 2.5)$ mm was accompanied by the extension of frequency tuning range to 27 GHz $< f < 32.5$ GHz and reduction of failures in Q_{load} throughout the tuning range. At the shift $s = 2.5$ mm there was also observed the increase in parameter β on frequencies $f < f_{MCP}$ (Fig. 9(c)).

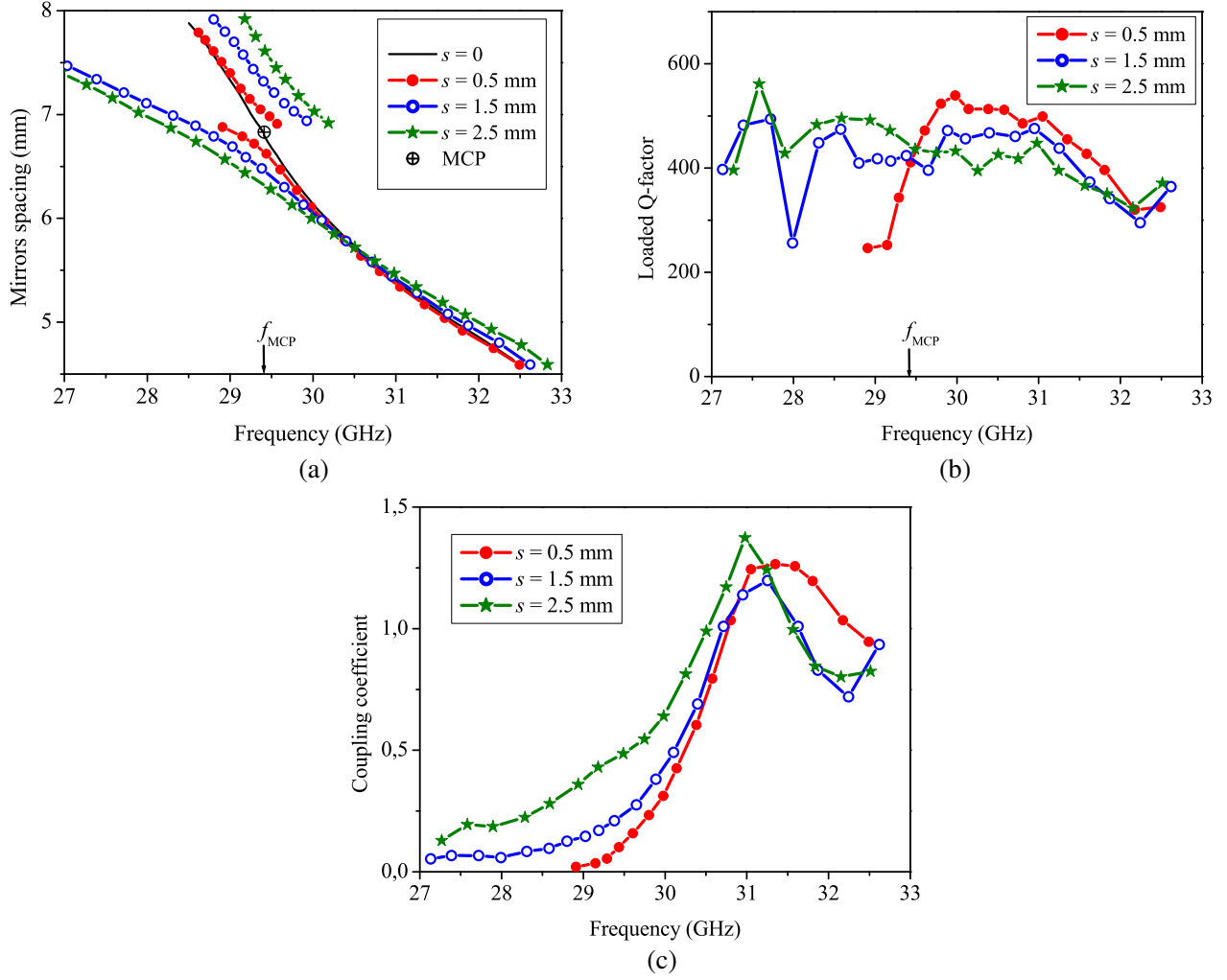


Figure 9. The “old” test results of the ORS with reflective double comb and $s = (0.5 \div 2.5)$ mm, operating on the mutual coupled modes $TEM_{002} \leftrightarrow TEM_{101}$: (a) dispersion diagram; (b) the ORS loaded Q-factor at tuning on the lower branch; (c) the ORS coupling coefficient at tuning on the lower branch.

The “hot” test of DRO, operating on the mutual coupled modes, was carried out on the prototype of the oscillator, which was under continuous vacuum pumping [15]. The flat mirror aperture was 52×32 mm², double comb parameters: $a = 5.58$ mm, $b = 10.0$ mm, $l = 1.0$ mm, $d = 0.5$ mm, $\delta = 0.2$ mm. The beam cross section dimension was $S_{beam} = 3.8 \times 0.12$ mm². The axis of the electron beam was set on the half-height of the channel in the double comb along OZ (Fig. 1). At the magnetic field level $B = 0.5$ T, the current transmission of the beam in the transit channel was 85%.

Using the focusing mirror of curvature radius $R_{sph} = 22.5$ mm and round aperture of diameter $2A = 28$ mm in the DRO prototype (at shift $s = 2.5$ mm), we obtained the generation on the lower and upper branches of mutual coupled modes $TEM_{002} \leftrightarrow TEM_{101}$. The minimum starting current at DRO operating on the lower branch of the mutual coupled modes was $I_{start} = 70$ mA. And the minimum starting current at DRO operating on the upper branch of the mutual coupled modes was $I_{start} = 35$ mA. At the operating starting current $I = 120$ mA and accelerating voltage for the electron beam $U = 2.7$ kV, the maximum output power of DRO on the lower branch of the mutual coupled modes was $P = 17$ W, and on the upper branch it was $P = 7.5$ W. The reason of decreasing of starting current and output power in DRO operating on the upper branch is a small coupling coefficient of the ORS ($\beta \approx 0.04$) at the coupling slot placement in the center of the spherical mirror.

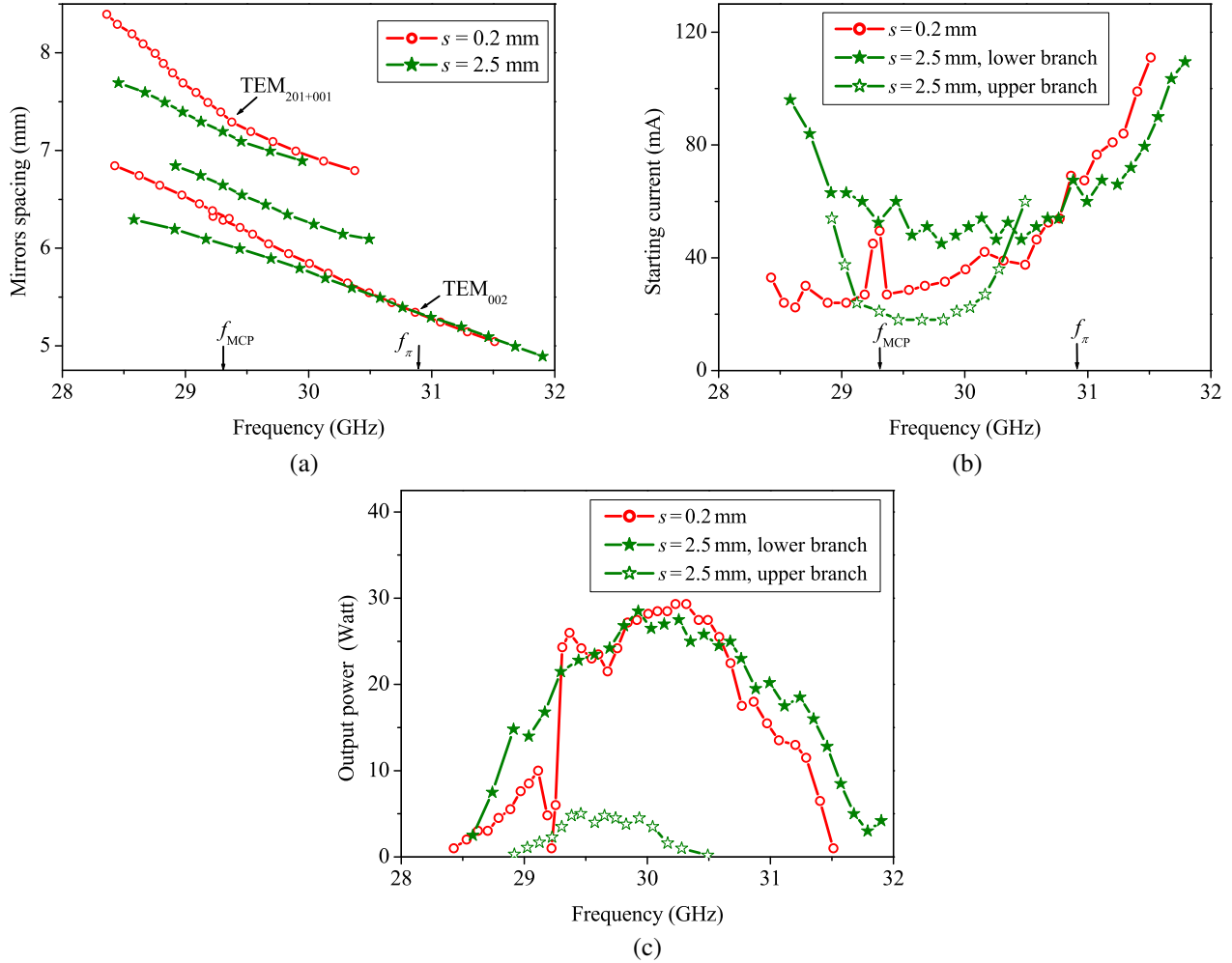


Figure 10. The “hot” test results of the DRO operation on the mutual coupled modes $TEM_{002} \leftrightarrow TEM_{101}$ at $s = 0.2$ mm and $s = 2.5$ mm: (a) dispersion diagram of excited modes in DRO; (b) starting current of DRO versus f ; (c) the DRO output power versus f .

To decrease the starting currents in DRO, operating on the mutual coupled modes $TEM_{002} \leftrightarrow TEM_{101}$, we used the focusing mirror with curvature radius $R_{sph} = 50$ mm and aperture 40×30 mm². This allowed to extend the interaction space length to $L = 2\omega_0 = 15$ mm. The dispersion curves for the modes, which were excited in DRO at intermirror distance 4.75 mm $< D < 8.5$ mm, are shown on Fig. 10(a). At a slight shift ($s = 0.2$ mm) between mirrors symmetry planes the frequency tuning in DRO was observed on TEM_{002} and $TEM_{201+001}$ modes. The local interaction between TEM_{002} and TEM_{101} modes was observed at $f_{MCP} = 29.30$ GHz, $D_{MCP} = 6.30$ mm.

When the shift was increased to $s = 2.5$ mm, the oscillator had a frequency tuning both on lower and upper branches of mutual coupled modes $TEM_{002} \leftrightarrow TEM_{101}$. Apparently, the higher-order $TEM_{201+001}$ mode came into mutual coupling with the TEM_{301} mode that led to slope decline of its dispersion curve (Fig. 10(a)).

At the excitation of oscillations in DRO with $R_{sph} = 50$ mm and $s = 2.5$ mm on the lower branch of the mutual coupled modes $TEM_{002} \leftrightarrow TEM_{101}$ the minimum starting current was $I_{start} = 45$ mA. The minimum starting current on the upper branch was $I_{start} = 18$ mA and that was even lower than in DRO with slight shift ($s = 0.2$ mm) between mirrors symmetry planes (Fig. 10(b)).

When DRO operated on the lower branch of the mutual coupled modes $TEM_{002} \leftrightarrow TEM_{101}$, the symmetric extending of the frequency tuning range was observed and the failures in output power disappeared. At the operating current $I = 120$ mA, the maximum output power of DRO on the lower

branch was $P = 30$ W. It was almost the same as the maximum output power in DRO with a slight shift ($s = 0.2$ mm) between mirrors symmetry planes (Fig. 10(c)). The frequency tuning range of the upper branch of the mutual coupled modes was $29 \text{ GHz} < f < 30.5 \text{ GHz}$ and the output power level didn't exceed $P = 4.5$ W.

4. CONCLUSIONS

For the first time, the DRO with frequency tuning on the mutual coupled modes that occurs in the ORS due to the shift between the mirrors symmetry planes, was developed and experimentally tested. The analysis of the mutual coupled modes features by using the rigorous 2-D model of the ORS has been carried out. For the partial frequencies calculation of the mutual coupled modes the dispersion equation of quadratic form was proposed and tested, which includes spectral and non-spectral parameters of the ORS.

It was shown that if we purposefully create the conditions for mutual coupling between the operating TEM_{00q} -mode and TEM_{10q-1} -mode having a sufficiently high radiation Q-factor, it is possible to organize the tuning of DRO on the mutual coupled modes in a wide band of frequencies without the influence of the higher-order modes on output characteristics of the oscillator.

For DRO in K_a band using the 2-D model of the ORS, the analysis of radiation and ohmic losses of the mutual coupled modes $TEM_{002} \leftrightarrow TEM_{101}$ for several values of the shift width between the mirrors symmetry planes was conducted. The starting current of DRO at frequency tuning on both branches of the mutual coupled modes has been calculated.

It has been established that at the optimal shift between the mirrors symmetry planes ($s = 2.5$ mm), there is an increase in the ORS Q-factor at $f < f_{MCP}$ and the tuning range of the DRO, operating on the lower branch of the mutual coupled modes $TEM_{002} \leftrightarrow TEM_{101}$, extends.

The results of the 2-D simulation are confirmed by experimental data, obtained in "cold" and "hot" tests of the DRO prototype, operating on the mutual coupled modes $TEM_{002} \leftrightarrow TEM_{101}$.

REFERENCES

1. Shestopalov, V. P., *The Smith-Purcell Effect*, Nova Science Publishers. Inc., Commack, NY, 1998.
2. Korneenkov, V. K., V. S. Miroschnichenko, and B. K. Skrynnik, "Diffraction radiation oscillator for CW and pulsed operation," *Telecommunications and Radio Engineering*, Vol. 51, Nos. 6&7, 144–147, 1997.
3. Yang, J., Y. Kan, L. Yang, G. Deng, Z. Yin, and J. Ruan, "Design of 300 GHz diffraction radiation oscillator with double grating," *Proceedings of 2015 IEEE International Vacuum Electronics Conference (IVEC-2015)*, Beijing, 2015.
4. Kurin, V. G., B. K. Skrynnik, and V. P. Shestopalov, "Realization of intermode oscillations in open resonator of diffraction radiation generator," *Radiophysics and Quantum Electronics*, Vol. 36, No. 11, 779–784, 1993.
5. Miroschnichenko, V. S., "Competition and cooperation of modes in small-volume DRO with periodic structure of coupled grooved waveguides," *Telecommunications and Radio Engineering*, Vol. 68, No. 3, 231–245, 2009.
6. Hong, J. S., "Coupling of asynchronously tuned coupled microwave resonators," *IEE Proceedings — Microwaves, Antennas and Propagation*, Vol. 147, No. 5, 354–358, 2000.
7. Park, S., "Mechanism of two-resonant modes for highly resonant wireless power transfer and specific absorption rate," *Progress In Electromagnetics Research C*, Vol. 69, 181–190, 2016.
8. Shestopalov, V. P., and Y. V. Shestopalov, *Spectral Theory and Excitation of Open Structures*, The Institution of Electrical Engineering, London, UK, 1996.
9. Melezhik, P. N., A. Y. Poedinchuk, Y. A. Tuchkin, and V. P. Shestopalov, "Analytical nature of the vibrational mode-coupling phenomenon," *Soviet Physics Doklady*, Vol. 33, 420–423, 1988.
10. Kovalov, I. O. and V. S. Miroschnichenko, "The features of diffraction radiation oscillator operating on the 1st Gaussian mode of the open resonant system," *2016 IEEE International Young Scientists Forum on Applied Physics and Engineering (YSF-2016)*, Kharkiv, Ukraine, Oct. 10–14, 2016.

11. Demchenko, M. Y., V. K. Korneenkov, V. S. Miroshnichenko, A. E. Poedinchuk, Y. V. Svischov, and Y. A. Tuchkin, "An open resonator with a rectangular groove on the mirror: Theory and experiment," *Telecommunications and Radio Engineering*, Vol. 58, No. 1&2, 1–16, 2002.
12. Svezhentsev, A. Ye., V. S. Miroshnichenko, and G. A. E. Vandenbosh, "Fast H-waves in double comb infinite arrays," *Progress in Electromagnetics Research C*, Vol. 80, 119–129, 2018.
13. Revin, I. D., B. K. Skrynnik, A. S. Sysoev, O. A. Tret'yakov, and V. P. Shestopalov, "Linear theory of diffraction radiation oscillator," *Radiophysics and Quantum Electronics*, Vol. 20, No. 5, 524–533, 1977.
14. Miroshnichenko, V. S., P. N. Melezhik, and Ye. B. Senkevich, "An open resonance cell for millimeter wave dielectrometer applications," *Progress in Electromagnetics Research M*, Vol. 4, 47–65, 2008.
15. Miroshnichenko, V. S. and I. O. Kovalov, "Diffraction radiation oscillator with asymmetric open resonant system. Part 2. The hot test results of diffraction radiation oscillator," *Journal of Nano- and Electronic Physics*, Vol. 8, No. 2, 02034(8), 2016.